Regional and hemispheric influences on measured spring peroxyacetyl nitrate (PAN) mixing ratios at the Auchencorth UK EMEP supersite

Christopher S. Malley [a,b,*], J. Neil Cape [a], Matthew R. Jones [a], Sarah R. Leeson [a], Mhairi Coyle [a], Christine F. Braban [a], Mathew R. Heal [b], Marsailidh M. Twigg [a]

[a] NERC Centre for Ecology & Hydrology, Bush Estate, Penicuik, EH26 0QB, UK
[b] School of Chemistry, University of Edinburgh, David Brewster Road, Edinburgh, EH9 3JF, UK
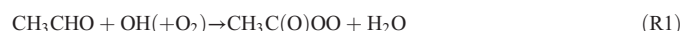
ARTICLE INFO

ABSTRACT

This work presents 15-min averaged measurements of peroxyacetyl nitrate (PAN) obtained during spring 2014 (24/04/2014 – 06/05/2014) at the Auchencorth UK EMEP supersite (southeast Scotland). The aim of this analysis was to investigate the conditions producing the distribution of PAN mixing ratios at the supersite in spring 2014. Air mass back trajectories showed the majority of air masses to have spent substantial time over the UK, continental Europe or Scandinavia prior to arrival at Auchencorth. The median and 95th percentile PAN mixing ratios observed were 0.46 ppb and 1.03 ppb, respectively. The median mixing ratio was elevated compared with previous PAN measurements during springtime (April–May) in southeast Scotland (corresponding median mixing ratios April–May 1994–1998: 0.1–0.3 ppb), which is hypothesised to be due to conditions conducive to regional (European) photochemical PAN production. Additionally, PAN mixing ratios during regionally influenced conditions (0.4–1.5 ppb) were substantially more elevated from hemispheric background mixing ratios (0.4–0.6 ppb) than for ozone (O_3, regional: 10–45 ppb, hemispheric: 30–40 ppb). PAN and O_3 both impact upon vegetation and human health and it is necessary to understand the extent to which hemispheric and regional processes contribute to their abundances in different locations. Regional processes can both increase and decrease PAN and O_3 mixing ratios compared to imported hemispheric background mixing ratios. This study concludes that during the measurement period in spring 2014 at the Auchencorth supersite, regional PAN and O_3 modifying processes enhanced PAN mixing ratios more than for O_3.

© 2016 Elsevier B.V. All rights reserved.

1. Introduction

Peroxyacetyl nitrate (PAN) is a secondary pollutant formed photochemically in aging air masses from the OH-initiated degradation of hydrocarbons, and combination with nitrogen dioxide (NO_2). For example, the oxidation of acetaldehyde followed by O_2 addition results in formation of the peroxyacetyl radical (PA), $CH_3C(O)O_2$ (R1). The reaction of PA with NO_2 forms PAN (R2) (Seinfeld and Pandis, 2006). This reaction is reversible and PAN can thermally decompose back to PA and NO_2, which can result in a PAN sink through the reaction of PA with NO (R3). However, at low temperatures PAN can be transported long distances, and provide a source of NO_2 in regions remote from NO_2 emissions sources. Hence PAN plays an important role in determining the spatial distribution of ozone (O_3) across the globe (Fischer et al., 2014). PAN has been shown to be a constituent of surface air in a variety of locations, including urban (Grosjean, 2001), rural (Brice et al., 1984;

McFadyen and Cape, 2005; Pandey Deolal et al., 2013) and remote (Beine and Krognes, 2000; Dassau et al., 2004):

$$CH_3CHO + OH(+O_2) \rightarrow CH_3C(O)OO + H_2O \quad (R1)$$

$$CH_3C(O)OO + NO_2 \rightleftarrows CH_3C(O)OONO_2(PAN) \quad (R2)$$

$$CH_3C(O)OO + NO \rightleftarrows CH_3 + CO_2 + NO_2 \quad (R3)$$

The last continuous measurements of PAN in the UK were conducted between 1994 and 1998 at Bush, southeast Scotland (McFadyen and Cape, 2005), although shorter campaign measurements have been conducted more recently (Hopkins et al., 2006; Lee et al., 2006). Between 1994 and 1998 at Bush, weekly averaged PAN mixing ratios peaked in spring (0.3 ppb), then decreased in summer to a minimum in winter (<0.1 ppb). At other monitoring sites, both PAN mixing ratios in air with minimal influence from European emissions, defined here as hemispheric background PAN mixing ratios (Beine et al., 1996; Pandey Deolal et al., 2013), and PAN mixing ratios in air transported from the

European boundary layer, show a peak in spring (Pandey Deolal et al., 2013, 2014). The relative scarcity of rural PAN measurements in the UK and Europe, and the substantial decrease in European PAN precursor emissions since the 1990s (EEA, 2014), were the motivation for these new measurements of PAN mixing ratios during late April/early May 2014 at the Auchencorth monitoring 'supersite' in southeast Scotland. The aim of this work was to determine the factors influencing the distribution of PAN mixing ratios arriving at Auchencorth in spring, and the conditions which produced the highest PAN mixing ratios. A variety of air masses were experienced permitting evaluation of contrasts between Arctic back trajectories (hemispheric background mixing ratios) and those passing over significant PAN precursor emissions sources (regional background mixing ratios), shown previously to be a key determinant of PAN levels across the UK and Europe (Brice et al., 1984; McFadyen and Cape, 1999a, 1999b; Pandey Deolal et al., 2014).

In addition, the covariance of PAN with NO_2 and O_3, two atmospheric constituents closely coupled to PAN (see, for example, Jenkin and Clemitshaw, 2000, and Atkinson, 2000), was also assessed across the measurement period. Both PAN and O_3 are determined by processes occurring on hemispheric, regional and local scales (Fischer et al., 2014; Jenkin, 2008; Lee et al., 2013) and are associated with negative impacts on health and vegetation (Monks et al., 2015; Teklemariam and Sparks, 2004; Vyskocil et al., 1998). It is therefore necessary to determine to what extent hemispheric, regional and local processes contribute to PAN and O_3 mixing ratios in different locations so that mitigation strategies can be effectively developed. Many studies have assessed the relative contributions of hemispheric, regional and local processes in determining O_3 mixing ratios across the UK (Jenkin, 2008; Malley et al., 2015a, 2015b; Munir et al., 2013), but sparse measurements have limited analogous assessments for PAN. Hence comparison of PAN and O_3 mixing ratios during different air masses at Auchencorth places the PAN variation in the context of a chemically related, and substantially more studied, atmospheric component.

2. Experimental

2.1. Fieldsite description

Auchencorth Moss is an ombrotrophic peat bog located in southeast Scotland, 17 km from the city of Edinburgh. Continuous measurement of 120 atmospheric constituents has taken place at the site since 2006, and Auchencorth is one of two European Monitoring and Evaluation Program (EMEP) 'supersites' in the UK (Torseth et al., 2012), as well as a regional Global Atmosphere Watch (GAW) site. The site has been described in detail previously (Cape et al., 2012; Twigg et al., 2015) and was shown to be representative of rural north and west UK when placed in the context of 100 European monitoring sites on the basis of monthly diurnal O_3 variation (Malley et al., 2014).

2.2. Instrument

PAN mixing ratios were measured at 3-min intervals at Auchencorth between 24/04/2014 and 06/05/2014 using gas chromatography with electron capture detection (GC-ECD). This method has been used extensively for PAN measurement (Beine and Krognes, 2000; Brice et al., 1984; Dassau et al., 2004; Flocke et al., 2005; Hopkins et al., 2006; McFadyen and Cape, 2005; Pandey Deolal et al., 2013). The GC consisted of a sampling loop, inlet column and main analytical column maintained iso-thermally at 14 °C. Carrier and make-up gas were both purified oxygen-free nitrogen set at 175 kPa and 250 kPa, respectively. The ECD detector was operated in constant current mode at 45 °C with a current of 1 nA and pulse voltage of 50 V. The instrument was housed in a temperature controlled cabin, and air was sampled from a height of 3 m through a 1/4″ PTFE inlet line at a flow rate of approximately 100 cm³ min⁻¹. The inlet of the sampling line faced downwards and was sheltered by a rain shield.

For the first 156 s of the 180-s sampling cycle, air from the sampling line was pumped through the 1-cm³ stainless steel sampling loop. After 156 s and 12 s prior to sample injection, the air flow was stopped to allow the pressure in the sampling loop to equilibrate. A 1-cm³ air sample was then injected into the inlet column, then through to the main analytical column. After 12 s the injection valve was returned to its initial position, which resulted in carrier gas passing through the main column, and backwards through the inlet column, preventing any water vapour or more-retained species from entering the main column. With this setup, only oxygen, PAN, and any contaminants with short retention times were passed through to the main column. The air pump was also switched back on 12 s after injection and the cycle repeated. Under these settings, the chromatogram was dominated by a large oxygen peak and PAN was detected as a small peak on the trailing edge of this oxygen peak with a retention time of approximately 70 s.

Ozone and NO_2 are measured continuously at the supersite by, respectively, UV photometry (Thermo Fisher Analyser, 49C) and thermal methods (Thermo Fisher Analyser, 42CTL) using a gradient system which sequentially samples 5 measurement heights. Mixing ratios used for comparison with PAN measurements were measured at 2.02 m.

2.3. Calibration and data processing

To identify the retention time of the PAN peak, and for calibration, PAN of known mixing ratio was generated from the photolytic reaction of NO in excess acetone (Flocke et al., 2005; Pandey Deolal et al., 2013). Mixing ratios ranging from 20 ppb to 80 ppb were generated by dilution of 10 ppm NO with zero air. Fig. 1 shows the calibration plot used to convert peak area to PAN mixing ratio. The linear regression is offset from the origin by 10.9 peak area units. When zero air was passed over acetone in the presence of UV light, the resulting chromatogram featured a peak at 70 s with an area of 5.8 peak area units. The peak indicates the presence of NO in the zero air, or another contaminant, resulting in systematic offset from zero in the calibration plot. Second, at lower mixing ratios a shoulder peak on the tail of the PAN peak was evident, examples of which are as shown in Fig. 2 and is included in the calculation of peak area for these mixing ratios. The peak was less apparent at higher PAN mixing ratios. It was assumed that the offset from zero in the calibration plot was accounted for by these two factors, and Eq. (1) was used to convert peak areas to PAN mixing ratios. The uncertainty in the estimated PAN mixing ratios introduced by the regression is ±4%, based on 95% confidence intervals.
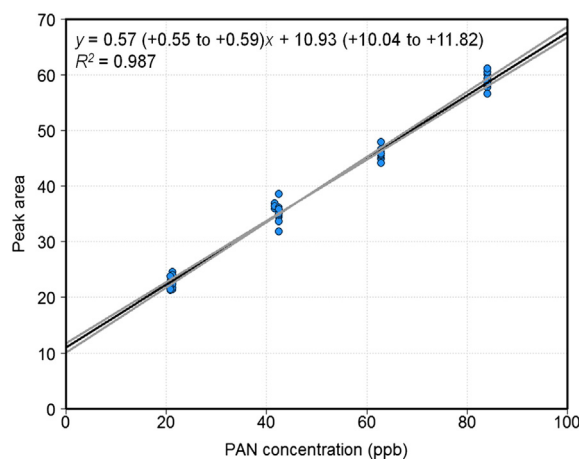
$$[PAN] = \frac{peak\ area}{0.57} \tag{1}$$

Fig. 1. Peak areas for known PAN mixing ratios (generated from the photolytic reaction of NO with excess acetone) used in the calibration of the GC-ECD method.
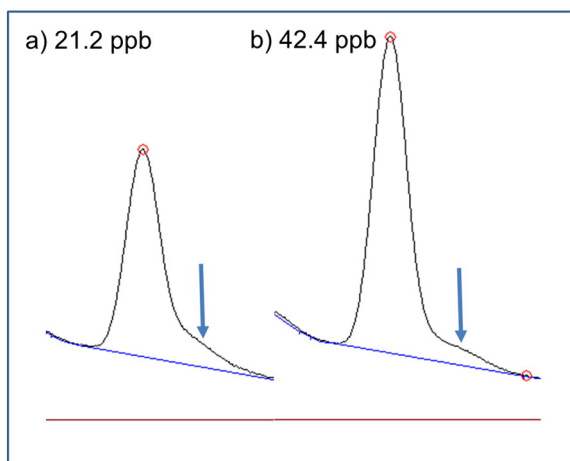
Fig. 2. Examples of the shoulder peak, indicated by blue arrows, in the chromatograms from the GC-ECD determination of (a) 20 ppb and (b) 40 ppb PAN calibration standards.

The limit of detection (LOD) of the method was calculated by identifying periods during which a substantial number of chromatograms had no PAN signal above noise (a non-detect). Table 1 summarises these time periods, along with the proportion of non-detects. Across all 7 time periods, 70% of observations were non-detects, accounting for 80% of all non-detects across the 13-day measurement period. The 30% of chromatograms with quantifiable 'PAN' peaks during these 7 periods were used as an estimate of the distribution of peak areas arising from false positive results. The 95th percentile of all these peaks was 0.19 peak area units, equivalent to 0.33 ppb, which means that the probability of falsely claiming PAN mixing ratios to be above the LOD was 0.05, in line with International Union of Pure and Applied Chemistry (IUPAC) recommendations (VIM, 2012). This definition of the LOD was a balance to minimise the probability of erroneously classifying false positive peaks as valid PAN mixing ratios, while simultaneously preserving as much valid PAN mixing ratio data as possible.

The 3-min data were aggregated to 15-min averages to reduce the influence of random variation in peak area. The 15-min averaging period was chosen to balance the need for repeat measurements to characterise random variation in peak area, while avoiding incorporation of atmospheric PAN mixing ratio variability. For inclusion in the time series, a minimum of 4 valid measurements were required during each 15-min interval. The maximum and minimum mixing ratio in each 15-min period was used as confidence intervals for the mean mixing ratio. The maximum PAN mixing ratios were on average 23% ± 8% higher than the minimum, and this random variation in peak areas was the largest source of uncertainty in the PAN mixing ratios (for comparison the uncertainty introduced by the calibration regression was ± 4%). Maximum-likelihood estimation (MLE) was used to fit a lognormal distribution to the 15-min PAN mixing ratios above 0.33 ppb, and confidence intervals for the mean and standard deviation of the MLE-derived distribution were calculated by bootstrap methods (Gardner, 2012; Helsel, 2006).

Table 1
Periods during the measurement campaign with a substantial proportion of non-detects.

Start date	End date	Number of observations	Percentage non-detects
24/04/14 00:00	24/04/14 11:56	239	83%
24/04/14 22:14	25/04/14 01:35	68	74%
28/04/14 23:41	29/04/14 00:32	18	44%
29/04/14 03:26	29/04/14 05:44	47	38%
03/05/14 02:01	03/05/14 06:16	86	33%
06/05/14 04:16	06/05/14 16:04	237	68%
06/05/14 21:19	06/05/14 23:58	54	57%

2.4. Back trajectories

To assess air mass origin, 96-h HYSPLIT three-dimensional air mass back trajectories (Draxler and Rolph, 2013) were calculated from the NCEP-NCAR Reanalysis meteorological data (Kistler et al., 2001) using the R statistical software package *Openair* (Carslaw and Ropkins, 2012; R Core Development Team, 2008). Trajectories were calculated for arrival at Auchencorth at each hour of each day. These trajectories were classified into four groups, 'northerly', 'easterly', 'southerly' and 'westerly' based on a visual assessment of the dominant direction taken by the air mass prior to arrival at Auchencorth (see Fig. 5 for examples). During the measurement period, those trajectories assigned to the northerly group were fast moving marine trajectories which spent little time over land. In the southerly group these trajectories were slower moving and spent the majority of time over the UK and France. Finally the trajectories assigned to the easterly group traversed both the UK, as well as continental Europe and/or Scandinavia, prior to arrival at Auchencorth. No trajectories during the measurement period were assigned as westerly air masses. The maximum height of each trajectory arriving at hourly intervals at Auchencorth during the measurement period varied from a maximum of 1464 m, and 95th, 75th and median values of 1254 m, 270 m and 125 m.

3. Results and discussion

3.1. PAN mixing ratios and dependence on air mass history

Across the 24/04–06/05/2014 monitoring period, 71% of the 1230 15-min intervals had sufficient valid measurements to report a PAN mixing ratio. Fig. 3 shows the cumulative distribution functions for the 15-min mean PAN mixing ratio data and the MLE-derived lognormal distribution (mean = −0.79, sd = 0.50) fitted to the data. The median mixing ratio during the measurement period was 0.46 ppb (median mixing ratios for MLE-derived lognormal distributions using minimum and maximum 15-min mixing ratios: 0.41 ppb and 0.49 ppb, respectively), the first and third quartiles were 0.33 ppb (0.30 ppb and 0.34 ppb)
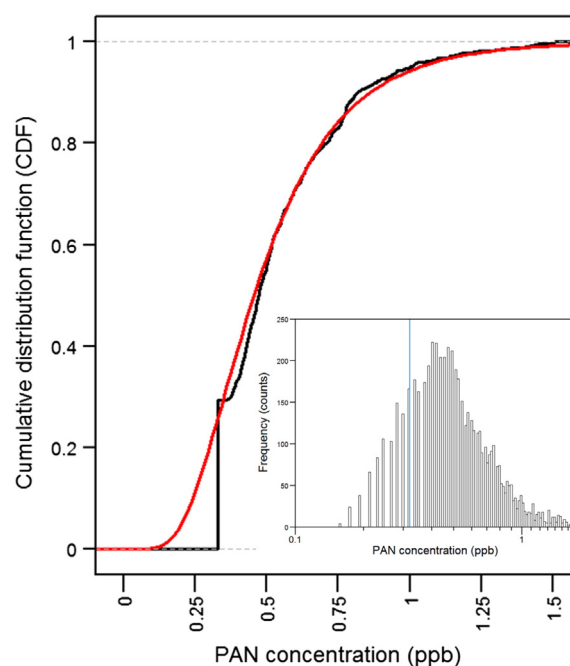

Fig. 3. Cumulative distribution functions of 15-min PAN mixing ratio data (black line) and theoretical lognormal distribution (red line) described by the mean = −0.79 and standard deviation = 0.50. Inset: histogram showing log-normal distribution of 3-min data including those values below 0.33 ppb LOD (blue line).
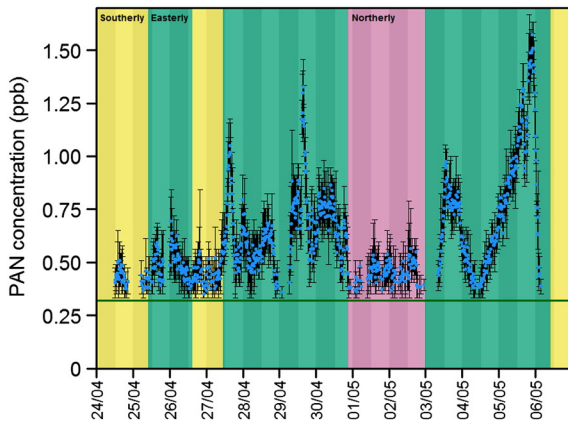
Fig. 4. Time series of 15-min averaged PAN mixing ratios. Whiskers indicate the maximum and minimum mixing ratios measured during that interval. Time periods where air mass back trajectories were northerly, easterly and southerly are denoted by pink, green and yellow background colours, respectively.

and 0.64 ppb (0.56 ppb and 0.72 ppb), respectively, and the 95th percentile was 1.03 ppb (0.88 and 1.23 ppb).

The time series of 15-min average PAN mixing ratios is shown in Fig. 4. The major variations in PAN mixing ratios across the measurement period are associated with changes in air mass origin, represented by 96-h back trajectories. On the 24/04 and the first half of 25/04, southerly air masses arrived at Auchencorth. The relatively small peak between 25 and 26/04 and the larger peak during the afternoon on 27/04 were associated with changes from southerly to easterly air masses (Fig. 5a). These easterly air masses arrived from higher latitudes compared to southerly air masses, resulting in lower temperatures along the trajectory pathway, reducing thermal decomposition of PAN,

while still traversing over PAN precursor emission source regions (Scandinavia and central/eastern Europe). Easterly air masses arrived during 28–30/04, and also travelled over the UK prior to arrival at Auchencorth. Under these conditions, daytime increases in PAN mixing ratios were evident (50% (0.22 ppb), and 220% (0.92 ppb) increase between daytime min and max on 28/04 and 29/04, respectively), with peak mixing ratios in excess of 1 ppb on 29/04 (Fig. 5b). Mixing ratios peaked in the afternoon between 15:00 and 17:00, indicating daytime photochemical production of PAN along the trajectory pathway, and mirroring patterns observed previously during daytime photochemical episodes (McFadyen and Cape, 1999b, 2005). Northerly, predominantly marine air masses arrived during 01–02/05 (Fig. 5c), resulting in lower mixing ratios, and little diurnal variability. The lack of emissions sources along the trajectory pathway inhibited photochemical PAN production during 01/05 and 02/05, but thermal decomposition of hemispheric background PAN mixing ratios would also be reduced due to the high latitude of the trajectory pathway. Finally, the remaining 2 peaks in PAN mixing ratios on the 03/05 and 05/05 were associated with a return to easterly air masses, which spent a substantial portion of time over the UK prior to arrival at Auchencorth (Fig. 5d).

While there are relatively few recent studies of PAN mixing ratios across the UK and Europe, previous rural PAN measurements (key statistics are summarised in Table 2) show those measured between 24/04/2014 and 06/05/2014 at Auchencorth to be substantially elevated from spring averages. The continuous measurements made at Bush, 7 km from Auchencorth and 15 km from Edinburgh on a common linear transect, between 1994 and 1998 were also log-normally distributed and annual average mixing ratios ranged from 0.085 to 0.117 ppb (McFadyen and Cape, 2005). For April and May in 1994 to 1998, the 13-day (same time period as spring 2014 measurement period) rolling median PAN mixing ratios were higher than the annual averages, up to 0.33 ppb (McFadyen and Cape, 2005) (up to 0.4 ppb in 1999 (unpublished data from the same site)). In comparison, the
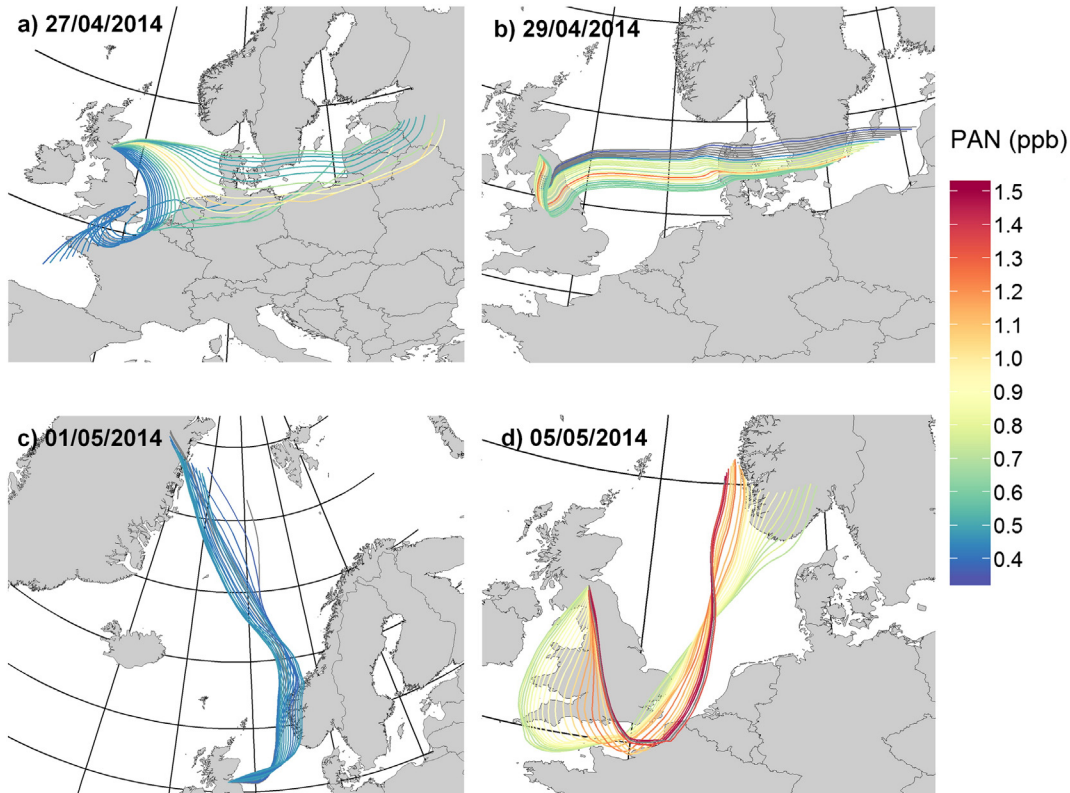

Fig. 5. Pathways of 96-hour air mass back trajectories arriving at the sampling site during each hour of (a) 27/04/2014 (southerly and easterly air masses), (b) 29/04/2014 (easterly air masses), (c) 01/05/2014 (northerly air masses) and (d) 05/05/2014 (easterly air masses). The colour of the trajectory is the average PAN mixing ratio during the hour of trajectory arrival at Auchencorth.

Table 2

Summary of previous rural and remote PAN measurements and key statistics to aid comparison with the measurements presented here at Auchencorth in spring 2014.

Site name	Location	Time period	Relevant PAN statistics	Reference
Auchencorth	Southeast Scotland, UK, rural	24/04–06/05/2014	Median: 0.41–0.49 ppb 95th percentile: 0.88–1.23 ppb	This study
Bush	Southeast Scotland, UK, rural	1994–1998	Spring weekly average: 0.15–0.32 ppb May 1995 photochemical episode: max 1.2 ppb	McFadyen and Cape (2005)
Great Dun Fell	Northwest England, UK, rural	Mar-Apr 1995	Arctic air masses: 0.2–0.5 ppb Polluted UK air masses: max 1.6 ppb	McFadyen and Cape (1999a)
Weybourne	Southeast England, UK, rural	Oct/Nov 1994 & Jun 1995	Polluted European air Oct 1994: max 1.2 ppb Polluted UK air Jun 1995: max 1.4 ppb	McFadyen and Cape (1999b)
Writtle, Essex	Southeast England, UK, rural	Aug 2003	Daytime av.: 0.24 ppb Daytime heatwave av.: 0.65 ppb August 2003 max: 1.6 ppb	Lee et al. (2006)
Flight campaign	Southeast England, UK, rural	18/08/2005	Flying over land (500 m) av.: 0.7 ± 0.2 ppb	Hopkins et al. (2006)
Zeppelin Observatory	Svalbard, Arctic, remote	1994–1996	Spring maximum: 0.4–0.5 ppb	Beine and Krognes (2000)
Jungfraujoch	Switzerland, Alpine site (3580 m),	1997–1998 and 2008–2010	Apr/May monthly av.: 0.3–0.5 ppb May 2008 air influenced by European boundary layer: max 1.2 ppb	Pandey Deolal et al. (2014)
Zugspitze	Austria, Alpine site (2670 m),	2004–2008	Apr/May monthly av.: 0.3–0.5 ppb May 2008 air influenced by European boundary layer: max 0.9 ppb	Pandey Deolal et al. (2014)
Hohenspeissenberg	Southern Germany, rural	2003–2006	Apr/May monthly av.: 0.3–0.8 ppb	Pandey Deolal et al. (2014)

median mixing ratio measured at Auchencorth in spring 2014 was 0.46 ppb. The peak PAN mixing ratios at Auchencorth in 2014 (maximum 15-min mixing ratio = 1.57 ppb (1.49–1.63), 95th percentile = 1.03 ppb, Fig. 4) were comparable to those measured during regional photochemical episodes in spring between 1994 and 1998 at Bush (e.g., in May 1995, PAN peaked at 1.2 ppb (McFadyen and Cape, 2005), and in spring 1998 hourly PAN peaked at 2.1 ppb (unpublished data)). Short-term monitoring studies at other rural UK sites showed that highest PAN mixing ratios were associated with air mass pathways which passed over the UK and Europe, for example, ground-based studies at Weybourne (eastern England, McFadyen and Cape (1999b)) and Great Dun Fell (northwest England, McFadyen and Cape (1999a)), and a flight campaign across southeast England (Hopkins et al., 2006). See Table 2 for relevant peak PAN mixing ratio statistics for each study.

More recently in Europe, monthly mean PAN mixing ratios in spring at Jungfraujoch, in the Swiss Alps, were between 0.3 ppb and 0.5 ppb between 2008 and 2010. There may be additional variability (both higher and lower) in PAN mixing ratios at Jungfraujoch when averaged over time periods equivalent to the measurement period in this study (13 days), which is not reflected in the monthly average mixing ratios. Jungfraujoch is a high-altitude alpine site (3470 m) where atmospheric composition is affected by both air masses from the free troposphere and the European planetary boundary layer (PBL) (Pandey Deolal et al., 2013). Highest mixing ratios at Jungfraujoch were measured in air which had had significant contact with the European PBL during

favourable photochemical production conditions, including the three-hourly maximum values of 1.2 ppb in May 2008 (Pandey Deolal et al., 2014). High hourly mixing ratios in spring were also measured at another alpine site, Zugspitze (Pandey Deolal et al., 2014) (Table 2). Atmospheric composition at these sites is more frequently determined by long-range transport of continental emissions compared with Auchencorth, and colder temperatures at the higher altitudes reduce thermal decomposition of PAN. The current extent of continuous PAN monitoring across Europe (4 sites across Switzerland, Austria and Germany) is insufficient to place the campaign measurements at Auchencorth in the full context of European PAN mixing ratio variation. Nevertheless, results from the alpine sites and previous UK short-term measurements demonstrate that high mixing ratios are experienced at other sites across Europe, which, given the correct meteorological conditions, can also affect rural UK sites such as Auchencorth. Additionally, measurements at a remote Arctic site between 1994 and 1997 recorded spring daily median PAN mixing ratios peaking between 0.4 and 0.5 ppb (Beine and Krognes, 2000), similar to the measurements at Auchencorth during the arrival of northerly, marine air (Fig. 4).

3.2. Comparison of PAN, O_3 and NO_2

The relationship between PAN mixing ratios and concurrent measurements of O_3 and NO_2 during the arrival of air masses from different major sectors is shown in Fig. 6. During northerly conditions
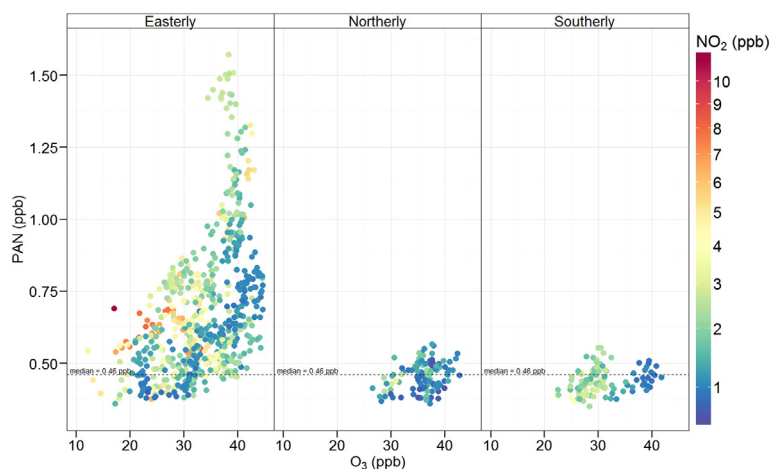

Fig. 6. Scatter plot for PAN and O_3 mixing ratios between 24/04/2014 and 06/05/2014 during different dominant air mass pathways with points coloured according to the measured NO_2 mixing ratio.

(e.g., during 01–02/05), mixing ratios of PAN (<0.53 ppb) and NO_2 were relatively low, and O_3 mixing ratios had little variability (generally between 30 and 40 ppb). During southerly conditions, PAN mixing ratios were again relatively low (<0.57 ppb), but O_3 mixing ratios were more variable and dependent on local NO_2 mixing ratio. The depletion of O_3, relative to the hemispheric background, of 10–15 ppb were associated with NO_2 mixing ratios up to 4 ppb. Low PAN mixing ratios during southerly conditions may result from lower emissions of PAN precursors along the trajectory pathway compared to easterly conditions, and higher temperatures at lower latitudes increasing the rate of thermal decomposition. The largest variability in PAN and O_3 mixing ratios was during the arrival of easterly air masses, which were the major air mass pathway during the measurement period, and there was a less obvious correlation of PAN and O_3 mixing ratios with NO_2 mixing ratios.

Northerly air masses were representative of hemispheric background PAN and O_3 mixing ratios with little influence from regional or local processes. Both hemispheric background O_3 (Derwent et al., 2013; Parrish et al., 2013) and PAN (Beine and Krognes, 2000; McFadyen and Cape, 2005; Pandey Deolal et al., 2013) have been shown to peak in spring. The southerly conditions had a larger contribution from local processes compared to northerly conditions, resulting in O_3 depletion due to elevated local NO_2. Easterly air masses spent a larger proportion of time travelling over the UK, continental Europe and Scandinavia, i.e., regions with PAN and O_3 precursor emissions sources (EEA, 2015), and hence there was a substantially larger contribution from regional emissions and chemical transformation than during northerly and southerly conditions. Regional processes can both increase and decrease PAN and O_3 mixing ratios relative to imported hemispheric background mixing ratios: PAN and/or O_3 mixing ratios can increase through regional photochemical production and can decrease through thermal dissociation (for PAN), chemical destruction by reaction with NO (for O_3) and deposition (for both). During the conditions with this regional component over the measurement period, PAN and O_3 production and destruction processes were more heavily in favour of production for PAN than for O_3. Hence, PAN mixing ratios during easterly conditions were substantially more elevated above hemispheric background compared with O_3 mixing ratios, and were determined to a greater extent by regional processes. For example, during the peaks in PAN mixing ratio on 27/04, 29/04, 03/05 and 05/05, PAN/O_3 ratios were 56%, 75%, 69% and 150% higher than the median for the measurement period, respectively. In addition, the average PAN mixing ratios during easterly conditions were 47% higher than during northerly conditions, while the average O_3 mixing ratios were 10% lower, and maximum easterly O_3 mixing ratios were only 28% higher than average northerly mixing ratios, compared to 306% higher for maximum easterly PAN mixing ratios.

During easterly conditions, there was low correlation between O_3 or PAN and NO_2. This results from variation in the relative contribution of regional and local processes in determining atmospheric composition during the campaign as O_3 and PAN are derived from regional and local modification of hemispheric background mixing ratios, while NO_2 is determined to a greater extent by local sources. For example, on 28/04, there was a large daytime peak in NO_2 mixing ratios (approximately 8 ppb) in the afternoon, but a modest increase in PAN mixing ratios, indicative of an increase in contribution from a local NO_2 source, e.g., the city of Edinburgh, 17 km away. This also coincided with decreasing O_3 mixing ratios, potentially due to increased local depletion by reaction with NO. By contrast, during easterly conditions on 25/04, 29/04, 03/05 and 05/05, elevated PAN/NO_2 ratios occurred, when the peaks in PAN mixing ratios generally coincided with less pronounced peaks in NO_2 mixing ratios. During 01–02/05 (i.e., northerly conditions), PAN/NO_2 ratios were both higher and lower than the period median value, reflecting changes in local NO_2 levels during this period with little regional influence.

4. Conclusion

PAN mixing ratios measured in late April/early May 2014 at Auchencorth are consistent with previous measurements of high percentile spring mixing ratios in the UK during periods with substantial continental European and UK emission source influence. These high mixing ratios resulted from the coincidence of annual maximum hemispheric background PAN mixing ratios in spring with conditions conducive to elevated regional photochemical PAN production. In addition, thermal decomposition of PAN was reduced due to the relatively high latitude trajectory pathways, and a low NO_x environment. PAN and O_3 are both photochemically derived atmospheric components with deleterious impacts, and it is important to understand the relative contributions of hemispheric and regional processes in determining their levels at a site for the effective development of impact mitigation strategies. The results in this analysis indicate that in spring 2014 at the Auchencorth supersite, during periods of regional air mass influence, PAN mixing ratios were substantially more elevated above imported hemispheric background mixing ratios than for concurrent O_3 measurements.

References

Atkinson, R., 2000. Atmospheric chemistry of VOCs and NO_x. Atmos. Environ. 34, 2063–2101.

Beine, H.J., Krognes, T., 2000. The seasonal cycle of peroxyacetyl nitrate (PAN) in the European Arctic. Atmos. Environ. 34, 933–940.

Beine, H.J., Jaffe, D.A., Blake, D.R., Atlas, E., Harris, J., 1996. Measurements of pan, alkyl nitrates, ozone, and hydrocarbons during spring in interior Alaska. J. Geophys. Res. 101, 12613–12619.

Brice, K.A., Penkett, S.A., Atkins, D.H.F., Sandalls, F.J., 1984. Atmospheric measurements of peroxyacetylnitrate (PAN) in rural, South-East England: seasonal variations winter photochemistry and long-range transport. Atmos. Environ. 18, 2691–2702.

Cape, J.N., Coyle, M., Dumitrean, P., 2012. The atmospheric lifetime of black carbon. Atmos. Environ. 59, 256–263.

Carslaw, D.C., Ropkins, K., 2012. openair—an R package for air quality data analysis. Environ. Model. Softw. 27-28, 52–61.

Dassau, T.M., Shepson, P.B., Bottenheim, J.W., Ford, K.M., 2004. Peroxyacetyl nitrate photochemistry and interactions with the Arctic surface. J. Geophys. Res. 109. http://dx.doi.org/10.1029/2004jd004562.

Derwent, R., Manning, A., Simmonds, P., Gerard Spain, T., O'Doherty, S., 2013. Analysis and interpretation of 25 years of ozone observations at the Mace Head Atmospheric Research Station on the Atlantic Ocean coast of Ireland from 1987 to 2012. Atmos. Environ. 80, 361–368.

Draxler, R.R., Rolph, G.D., 2013. HYSPLIT (HYbrid Single-Particle Lagrangian Integrated Trajectory) Model Access via NOAA ARL READY Website (http://www.arl.noaa.gov/HYSPLIT.php) NOAA Air Resources Laboratory, College Park, MD.

EEA, 2014. EU emission inventory report 1990–2012 under the UNECE Convention on long-range transboundary air pollution (LRTAP). EEA technical report No 12/2014. European Environment Agency (http://www.eea.europa.eu//publications/lrtap-2014).

EEA, 2015. EU emission inventory report 1990–2013 under the UNECE Convention on long-range transboundary air pollution (LRTAP). EEA technical report No 8/2015. European Environment Agency (available at:http://www.eea.europa.eu//publications/lrtap-emission-inventory-report).

Fischer, E.V., Jacob, D.J., Yantosca, R.M., Sulprizio, M.P., Millet, D.B., Mao, J., Paulot, F., Singh, H.B., Roiger, A., Ries, L., Talbot, R.W., Dzepina, K., Deolal, S.P., 2014. Atmospheric peroxyacetyl nitrate (PAN): a global budget and source attribution. Atmos. Chem. Phys. 14, 2679–2698.

Flocke, F., Weinheimer, A., Swanson, A., Roberts, J., Schmitt, R., Shertz, S., 2005. On the measurement of PANs by gas chromatography and electron capture detection. J. Atmos. Chem. 52, 19–43.

Gardner, M., 2012. Improving the interpretation of 'less than' values in environmental monitoring. Water Environ. J. 26, 285–290.

Grosjean, D., 2001. Long-term trends in ambient peroxyacetyl nitrate in southern California. Abstr. Pap. Am. Chem. Soc. 221 (53-ENVR).

Helsel, D.R., 2006. Fabricating data: how substituting values for nondetects can ruin results, and what can be done about it. Chemosphere 65, 2434–2439.

Hopkins, J.R., Boddy, R.K., Hamilton, J.F., Lee, J.D., Lewis, A.C., Purvis, R.M., Watson, N.J., 2006. An observational case study of ozone and precursors inflow to South East England during an anticyclone. J. Environ. Monit. 8, 1195–1202.

Jenkin, M.E., 2008. Trends in ozone concentration distributions in the UK since 1990: local, regional and global influences. Atmos. Environ. 42, 5434–5445.

Jenkin, M.E., Clemitshaw, K.C., 2000. Ozone and other secondary photochemical pollutants: chemical processes governing their formation in the planetary boundary layer. Atmos. Environ. 34, 2499–2527.

Kistler, R., Kalnay, E., Collins, W., Saha, S., White, G., Woollen, J., Chelliah, M., Ebisuzaki, W., Kanamitsu, M., Kousky, V., van den Dool, H., Jenne, R., Fiorino, M., 2001. The NCEP-NCAR 50-year reanalysis: monthly means CD-ROM and documentation. Bull. Am. Meteorol. Soc. 82, 247–267.

Lee, J.D., Lewis, A.C., Monks, P.S., Jacob, M., Hamilton, J.F., Hopkins, J.R., Watson, N.M., Saxton, J.E., Ennis, C., Carpenter, L.J., Carslaw, N., Fleming, Z., Bandy, B.J., Oram, D.E., Penkett, S.A., Slemr, J., Norton, E., Rickard, A.R., Whalley, L.K., Heard, D.E., Bloss, W.J., Gravestock, T., Smith, S.C., Stanton, J., Pilling, M.J., Jenkin, M.E., 2006. Ozone photochemistry and elevated isoprene during the UK heatwave of August 2003. Atmos. Environ. 40, 7598–7613.

Lee, J.B., Yoon, J.S., Jung, K., Eom, S.W., Chae, Y.Z., Cho, S.J., Kim, S.D., Sohn, J.R., Kim, K.H., 2013. Peroxyacetyl nitrate (PAN) in the urban atmosphere. Chemosphere 93, 1796–1803.

Malley, C.S., Braban, C.F., Heal, M.R., 2014. The application of hierarchical cluster analysis and non-negative matrix factorization to European atmospheric monitoring site classification. Atmos. Res. 138, 30–40.

Malley, C.S., Heal, M.R., Mills, G., Braban, C.F., 2015a. Trends and drivers of ozone human health and vegetation impact metrics from UK EMEP supersite measurements (1990-2013). Atmos. Chem. Phys. 15, 4025–4042.

Malley, C.S., Braban, C.F., Dumitrean, P., Cape, J.N., Heal, M.R., 2015b. The impact of speciated VOCs on regional ozone increment derived from measurements at the UK EMEP supersites between 1999 and 2012. Atmos. Chem. Phys. 15, 8361–8380.

McFadyen, G.G., Cape, J.N., 1999a. Spring time sources and sinks of peroxyacetyl nitrate in the UK and its contribution to acidification and nitrification of cloud water. Atmos. Res. 50, 359–371.

McFadyen, G.G., Cape, J.N., 1999b. Physical and chemical influences on PAN concentrations at a rural site. Atmos. Environ. 33, 2929–2940.

McFadyen, G.G., Cape, J.N., 2005. Peroxyacetyl nitrate in eastern Scotland. Sci. Total Environ. 337, 213–222.

Monks, P.S., Archibald, A.T., Colette, A., Cooper, O., Coyle, M., Derwent, R., Fowler, D., Granier, C., Law, K.S., Mills, G.E., Stevenson, D.S., Tarasova, O., Thouret, V., von Schneidemesser, E., Sommariva, R., Wild, O., Williams, M.L., 2015. Tropospheric ozone and its precursors from the urban to the global scale from air quality to short-lived climate forcer. Atmos. Chem. Phys. 15, 8889–8973.

Munir, S., Chen, H., Ropkins, K., 2013. Quantifying temporal trends in ground level ozone concentration in the UK. Sci. Total Environ. 458, 217–227.

Pandey Deolal, S., Staehelin, J., Brunner, D., Cui, J., Steinbacher, M., Zellweger, C., Henne, S., Vollmer, M.K., 2013. Transport of PAN and NOy from different source regions to the Swiss high alpine site Jungfraujoch. Atmos. Environ. 103-115.

Pandey Deolal, S., Henne, S., Ries, L., Gilge, S., Weers, U., Steinbacher, M., Staehelin, J., Peter, T., 2014. Analysis of elevated springtime levels of Peroxyacetyl nitrate (PAN) at the high Alpine research sites Jungfraujoch and Zugspitze. Atmos. Chem. Phys. 14, 12553–12571.

Parrish, D.D., Law, K.S., Staehelin, J., Derwent, R., Cooper, O.R., Tanimoto, H., Volz-Thomas, A., Gilge, S., Scheel, H.E., Steinbacher, M., Chan, E., 2013. Lower tropospheric ozone at northern midlatitudes: changing seasonal cycle. Geophys. Res. Lett. 40, 1631–1636.

R Core Development Team, 2008. R: A Language and Environment for Statistical Computing. R Foundation for Statistical Computing, Vienna, Austria. ISBN 3-900051-07-0, (URL http://www.R-project.org).

Seinfeld, J.H., Pandis, S.N., 2006. Atmospheric Chemistry and Physics: From Air Pollution to Climate Change. Wiley-Blackwell.

Teklemariam, T.A., Sparks, J.P., 2004. Gaseous fluxes of peroxyacetyl nitrate (PAN) into plant leaves. Plant Cell Environ. 27, 1149–1158.

Torseth, K., Aas, W., Breivik, K., Fjaeraa, A.M., Fiebig, M., Hjellbrekke, A.G., Myhre, C.L., Solberg, S., Yttri, K.E., 2012. Introduction to the European Monitoring and Evaluation Programme (EMEP) and observed atmospheric composition change during 1972–2009. Atmos. Chem. Phys. 12, 5447–5481.

Twigg, M.D.M., Leeson, C.F., Dijk, S.van, Jones, N., Leith, M.R., Morrison, I.D., Coyle, E., Proost, M., Peeters, R., Lemon, A.N.M., Frelink, E., Braban, T., Nemitz, C.F., Cape, E., N., J., 2015. Water soluble aerosols and gases at a UK background site—part 1: controls of PM2.5 and PM10 aerosol composition. Atmos. Chem. Phys. 15, 8131–8145.

VIM, 2012. International vocabulary of metrology—basic and general concepts and associated terms (VIM). JCGM 200:2012. Joint Committee for Guides in Metrology (available at:http://www.bipm.org/en/publications/guides/vim.html).

Vyskocil, A., Viau, C., Lamy, S., 1998. Peroxyacetyl nitrate: review of toxicity. Hum. Exp. Toxicol. 17, 212–220.